# Life-Long Coral Skeletal Acclimatization at $CO_2$ Vents in Papua New Guinea Reveals Species- and Environment-Specific Effects

**Fiorella Prada**
Marine Science Group, Department of Biological, Geological and Environmental Sciences, University of Bologna
**Leonardo Brizi**
Department of Physics and Astronomy, University of Bologna
**Silvia Franzellitti**
Department of Biological, Geological and Environmental Sciences, University of Bologna
**Stefano Mengoli**
Department of Management, University of Bologna
**Simona Fermani**
Department of Chemistry 'Giacomo Ciamician', University of Bologna
**Iryna Polishchuk**
Department of Material Sciences and Engineering and the Russell Berrie Nanotechnology Institute, Technion – Israel Institute of Technology
**Nicola Baraldi**
Marine Science Group, Department of Biological, Geological and Environmental Sciences, University of Bologna
**Francesco Ricci**
School of BioSciences, University of Melbourne
**Quinzia Palazzo**
Department of Chemistry 'Giacomo Ciamician', University of Bologna
**Erik Caroselli**
Marine Science Group, Department of Biological, Geological and Environmental Sciences, University of Bologna
**Boaz Pokroy**
Department of Material Sciences and Engineering and the Russell Berrie Nanotechnology Institute, Technion – Israel Institute of Technology
**Loris Giorgini**
Department of Industrial Chemistry "Toso Montanari", University of Bologna
**Zvy Dubinsky**
The Mina and Everard Goodman Faculty of Life Sciences, Bar-Ilan University
**Paola Fantazzini**

Department of Physics and Astronomy, University of Bologna

**Giuseppe Falini**

Department of Chemistry ‘Giacomo Ciamician’, University of Bologna

**Stefano Goffredo** ( s.goffredo@unibo.it )

Marine Science Group, Department of Biological, Geological and Environmental Sciences, University of Bologna

**Katharina Fabricius**

Australian Institute of Marine Science

---

**Research Article**

**Keywords:** climate change, ocean acidification, skeletal parameters, intra-skeletal organic matrix and water content, morphological plasticity

**Posted Date:** January 5th, 2021

**DOI:** https://doi.org/10.21203/rs.3.rs-138498/v1



---

# Abstract

The responses of corals and other marine calcifying organisms to ocean acidification (OA) are variable and span from no effect to severe responses. Here we investigated the effect of long-term exposure to OA on skeletal parameters of four tropical zooxanthellate corals living at two $CO_2$ vents in Papua New Guinea, namely in Dobu and Upa Upasina. The skeletal porosity of *Galaxea fascicularis*, *Acropora millepora*, and *Pocillopora damicornis* was higher (from 17% to 38%, depending on the species) at the seep site compared to the control only at Upa Upasina. Massive *Porites* showed no differences at any of the locations. *Pocillopora damicornis* also showed a ~ 7% decrease of micro-density and an increase of the volume fraction of the larger pores, a decrease of the intraskeletal organic matrix content with an increase of the intraskeletal water content, and no variation in the organic matrix related strain and crystallite size. The fact that the skeletal parameters varied only at one of the two seep sites suggests that other local environmental conditions interact with OA to modify the coral skeletal parameters. This might also contribute to explain the great deal of responses to OA reported for corals and other marine calcifying organisms.


# 1. Introduction

Tropical coral reefs support the livelihoods of hundreds of millions of people around the world, harbor 25% of all marine species, and protect thousands of kilometers of shoreline from waves and storms [1]. However, coral reefs face a wide and intensifying array of threats deriving from pollution and overexploitation on centennial scales which is leading to a decline in their health [2]. In addition, global climate change compounds these threats in multiple ways. Declines in seawater pH and associated decreases in carbonate ion concentration driven by ocean acidification (OA) is projected to have profound implications for marine calcifiers, as carbonate ions are essential for biotic calcification [3]. Many biological features may affect coral responses to OA, such as colony morphology, skeletal mineralogy and structure, body size, tissue thickness, symbiont types, and/or the mechanisms of nutrient acquisition [4]. Moreover, the discrepancy among responses could derive from different experimental designs and analytical methods (e.g., addition of acid vs $CO_2$ bubbling to mimic OA), co-limiting environmental conditions (e.g., temperature, light intensity, flow, feeding, etc.), and exposure times (days to months or even life times) [5].

Most studies to date, both under controlled conditions in aquaria and under natural conditions in the field (e.g., $CO_2$ vents), support predictions of decreased rates of calcification and increased rates of dissolution and bioerosion as seawater pH decreases [6]. However, coral calcification rates recorded for several decades within skeletal cores indicate there hasn't been a constant decline as ocean pH decreased and temperatures warmed throughout the 20th century. On the contrary, at some locations calcifications rates have remained stable and in others they have increased over this time period [7,8]. Even where declines in calcification have occurred, many other factors such as ocean warming, sea level rise, changes in surface ocean productivity, as well as many localized anthropogenic disturbances that co-occur with OA and also influence coral growth obscure our ability to attribute such changes solely to OA [9].

Most of the available knowledge about OA effects on marine organisms derives from short-term laboratory or mesocosm experiments on isolated organisms [10], which can substantially underestimate full organism acclimatization [11]. In fact, taxa that result apparently unaffected by high $CO_2$ under controlled conditions may be: 1) vulnerable in the long-term [12], 2) affected during life stages that were not considered during the experiment [13], or 3) be indirectly affected by OA-driven ecological changes (e.g., food webs, competition, diseases and/or community structures, habitat properties such as microbial surface biofilms) [14]. Likewise, other taxa that respond negatively to OA under controlled conditions may be capable of acclimatizing in the longer term. Thus, field experiments, where organisms are naturally exposed to OA for their entire life, as found around submarine $CO_2$ vents, could provide important new insights. However, vent systems are not perfect predictors of future ocean ecology owing to temporal variability in pH, spatial proximity of populations unaffected by acidification, and the unknown effects of other changing parameters (e.g., temperature, currents) [15]. Nonetheless, vents acidify sea water on sufficiently large spatial and temporal scales to integrate ecosystem processes such as reproduction, competition and predation [16]. Field-based studies conducted at volcanic $CO_2$ seeps in Italy [16–18], Japan [19], Mexico [20], and Papua New Guinea (PNG) [14] provide a unique opportunity to investigate long-term effects of OA on marine ecosystems that have been naturally exposed to chronic low pH and concomitant altered carbonate chemistry parameters for years/decades. These studies have already demonstrated substantial changes in community structure and functional biodiversity [21] of benthic species, as well as an array of responses to OA spanning from sharp decrease to no effect on calcification rate [22]. Studies conducted on corals at volcanic $CO_2$ vents in PNG have supported the mixed effects observed in laboratory experiments [14,23]. Hard coral cover is similar at acidified and control sites (33% versus 31%). However, the cover of massive *Porites* corals doubled under OA, whereas the cover of more structurally complex corals is reduced by one third [23]. Some species are significantly less common or even absent under OA. For instance, while the coverage of *Pocillopora damicornis* decreases by 43% in acidified sites, *in situ* growth measurements have found small differences in linear extension rate [14], but large differences in recruitment success [24]. Population reductions *in situ*, combined with observations of negative physiological impacts, including declines in calcification under OA, strongly suggest that low pH imposes selection pressure on less resilient taxa within the PNG system [22].

The aim of this study was to assess the effects of long-term exposure to OA on the skeletal parameters (micro-density, porosity, bulk density) of four tropical zooxanthellate coral species *Galaxea fascicularis* (Linnaeus, 1767), *Acropora millepora* (Ehrenberg, 1834), massive *Porites* Link, 1807, and *P. damicornis* (Linnaeus, 1758), living at PNG $CO_2$ vents [14]. The study was conducted at two locations in Milne Bay Province, PNG, namely Upa Upasina and Dobu (Fig. 1). At each location, corals were collected from a shallow water (1–5 m) cool volcanic $CO_2$ vent (seep hereafter) and a control site. The algal endosymbionts of these corals did not differ between seep and control sites, nor between the two seep locations [25]. Seep and control sites have been characterized in detail [14,23].

# 2. Materials And Methods

# 2.1 Study sites and coral sampling

The study was conducted at two shallow-water (1–5 m) volcanic $CO_2$ seeps at ambient temperature and adjacent control sites at Milne Bay Province, PNG, namely Dobu and Upa Upasina (Fig. 1). Almost pure $CO_2$ (~ 99%) has been streaming from the seabed for an unknown period of time (confirmed for approximately 70 years, but possibly much longer) [14], resulting in localized acidified conditions. Environmental parameters were measured across a 4-year period (2010–2013) at 1–5 m depth in both control and seep sites at Dobu and Upa Upasina, as previously reported [14,23]. Two-cm coral fragments were collected at 1–5 m depth from adult colonies of *P. damicornis*, *G. fascicularis*, *A. millepora*, and Massive *Porites* at control and seep sites in Dobu and Upa Upasina in August 2010 (N = 6–15 fragments per site, each fragment from a different colony; Supplementary Table S1) in Dobu and Upa Upasina [25]. Tissue from the coral fragments was totally removed following standardized protocols [26].

# 2.2 Skeletal parameters determination

The skeletal paramaters of 192 fragments from the control and seep sites at Dobu and at Upa Upasina (6–15 for each site) were obtained by buoyant weight measurements with a hydrostatic balance (Ohaus Explorer Pro balance ± 0.0001 g) equipped with a density determination kit. After determining the dry mass the fragments were placed inside a dryer chamber connected to a vacuum pump to evacuate air and water from the pores. After 3 h, water was gently introduced to fully saturate the samples which were then weighed in air. The buoyant weight was then obtained by applying the density determination kit, and the skeletal parameters were calculated by means of standard calculations (details in Supplementary Methods; [26]).

# 2.3 Time-Domain Nuclear Magnetic Resonance for pore size distribution determination

This technique was used to investigate the 'pore-size' distribution of *P. damicornis* coral skeletal fragments from each control and seep site (details in Supplementary Methods). Each coral fragment was saturated with distilled water, then removed from the water and placed on a wet paper to dry the excess of water on its surface. Then, every fragment was put inside a glass tube, sealed and measured. A home-built relaxometer based on an electromagnet JEOL C-60 operating at 0.5 T with a coil ≈ 8 mm in diameter, and equipped with a Spinmaster portable console (Stelar, Mede, Pavia, Italy) was used. The Carr- Purcell-Meiboom-Gill (CPMG) sequence with 200 µs echo time was used for $T_2$ measurements. The measured multi-exponential relaxation curves, affected by unavoidable measurement noise, were transformed into $T_2$ distributions by the algorithm UPEN (Uniform-Penalty inversion algorithm) [27], implemented in UpenWin. The ratio between the NMR signal under a particular portion of the distribution and the total NMR signal will correspond to the ratio of the volume of the pores with a particular pore size to the total pore volume, giving, as an example, the macro-scale pore fraction. A total of 60 fragments from the control and seep sites at Dobu (15 for each site) and at Upa Upasina (15 for each site) were analyzed.

## 2.4 Thermogravimetric Analysis for organic matrix content determination

Thermal gravimetric measurements were performed on using a TA Instruments thermobalance model SDT-Q600 with 0.1 µg of balance sensitivity. Powdered samples (5 to 10 mg), held in alumina

pans, were heated under a linear gradient from ambient (ca. 20 °C) up to 600 °C with an an isotherm at 120 °C for 5 min to remove the adsorbed water; heating rate: 10 °C/min under an $N_2$ atmosphere, with flux fixed to 100 ml/min. Two main weight loss regimes were identified: a first one in a range around 125–250° C (related to the loss of structured water molecules) followed by another thermal region between 250 °C and 470° C (generally associated with organic matrix pyrolysis) [28]. A total of 32 fragments from the control and seep sites at Dobu (10 for each site) and at Upa Upasina (6 for each site) were analyzed. Before the analysis the baseline and temperature were calibrated.

## 2.5 Synchrotron high-resolution X-ray powder diffraction

The coral fragments were measured at the ID22 beamline of the European Synchrotron Radiation Facility (Grenoble, France) using a wavelength of 0.4 Å (details in Supplementary Methods). The fragments were air-dried and ground with an agate mortar and pestle to a fine powder which was then loaded into borosilicate glass capillaries of 0.7–1 mm in diameter and measured at room temperature and after ex-situ heating at 300 °C for 2 h. A Rietveld refinement was used to calculate the unit-cell parameters of the diffraction pattern profiles. The line profile analysis was applied to a specific diffraction peak to obtain the coherence length (nm) along various crystallographic directions, which was achieved by fitting the profile to a Voigt function and deconvoluting the Lorentzian and Gaussian widths. Analyses were conducted on fragments of *P. damicornis* from Upa Upasina in the control (N = 3) and seep (N = 3) site.

## 2.6 Statistical analyses

Skeletal parameters (including macro-scale pore fraction, water content and organic matrix content analysed in *P. damicornis*) were compared between control and seep sites using the non-parametric Kruskal-Wallis test ($\chi^2$), due to deviations from parametric ANOVA assumption being verified (Normality: Shapiro-Wilk's test; equal variance: Bartlett's test). Statistical analyses were performed using SPSS 20.0. Data visualization, and graphics were obtained with the ggplot2 R package in R [29]. Statistical differences were accepted when $p < 0.05$.

Permutation multivariate analysis of variance (PERMANOVA) were perfomed using PRIMER v6 [30] and based on Euclidean distances (999 permutation) to test for (i) variations of environmental parameters amongst locations and sites, and across seasons; (ii) variations of skeletal parameters amongst locations, sites, and species. When the main tests revealed statistical differences ($p < 0.05$), PERMANOVA pairwise comparisons were carried out. Distance-based redundancy linear modeling (DISTLM) with a test of marginality in PRIMER was also performed to account for the contributions environmental parameters in explaining the total observed variance in the skeletal parameter datasets of each species. DISTLM used the BEST selection procedure and adjusted $R^2$ selection criteria. BEST BIOENV routine in PRIMER 6 was also

carried out to explain the observed patterns of nano-, mico- and macro-scale paraemetrs of *P. damicornis* (999 permutations). BEST BIOENV method performs permutation tests on environmental variables for determining which subset of variables produced the highest correlation with biological data. The environmental and biological data matrices were used to calculates a Spearman's rank correlation coefficient between these two matrices.

# 3. Results

## 3.1. Environmental parameters

The complete dataset of environmental parameters was analyzed to test for the differences between sampling locations, and, within each location, for control *vs* seep sites. Effects of seasonality were also considered. PERMANOVA analyses (Supplementary Table S2) show that the locations (Dobu *vs* Upa Upasina, regardless of sites) differed for temperature and DIC ($p < 0.01$; Supplementary Table S2 and Fig. S1), while control and seep sites within both locations differed for carbonate chemistry parameters ($p < 0.01$), while sharing the same temperature (Table 1; Supplementary Table S2). Salinity resulted significantly lower at the seep site compared to the control in Upa Upasina (Table 1). Significant seasonal variations were observed only for aragonite saturation state ($\Omega_{AR}$) ($p < 0.05$; Supplementary Table S2 and Fig. S1).

Controls at the two locations displayed lower pH and higher DIC, total alkalinity, salinity, and temperature at Upa Upasina compared to Dobu, while $pCO_2$ and $\Omega_{AR}$ did not change. Seep sites at the two locations showed higher pH, $\Omega_{AR}$, total alkalinity, and temperature, and lower $pCO_2$, DIC at Upa Upasina compared to Dobu, while salinity did not change (Table 1).

DISTLM analysis and the related tests of marginality indicate that carbonate chemistry parameters (i.e., $pCO_2$, $pH_{TS}$, and $\Omega_{AR}$) explained most of the variance observed in the environmental dataset (Fig. 2A). Indeed, PCO analyses show that these parameters are those that mostly explained the differences between controls and seeps within the two locations (Fig. 2B), while temperature and DIC seem to explain the differences between the two locations (Fig. 2B).

## 3.2. Skeletal parameters in corals from control and seep sites at the two locations

Variations of the skeletal parameters bulk density, micro-density, and porosity are reported in Fig. 3 and in Supplementary Table S1. In all four species, none of these skeletal parameters were affected by $CO_2$ at Dobu ($p > 0.05$). At Upa Upasina, *A. millepora* and *G. fascicularis* showed significantly higher porosity (+ 38% and + 25%, respectively) and consequently lower bulk density (− 13% and − 15%, respectively) in the seep compared to the control site (Fig. 3A,B; Supplementary Table S1). At the same location, *P. damicornis* showed significant variation in all investigated skeletal parameters, with lower micro-density (− 7%), higher porosity (+ 17%), and lower bulk density (− 12%) at the seep compared to the control site (Fig. 3C; Supplementary Table S1). Skeletal parameters in massive *Porites* did not change between seep and control sites in either locations (Fig. 3D; Supplementary Table S1). PERMANOVA analyses confirmed Site as a

significant factor determining the observed variations in porosity and bulk density, while also accounting for the significant species-specific variations in all skeletal parameters (Supplementary Table S3). Furthermore, porosity and bulk density also showed a significant interaction between Location and Site, while micro-density showed a significant interaction between Site and Species (Supplementary Table S3).

The decreased micro-density in *P. damicornis* between seep and control sites at Upa Upasina was further explored to assess additional macroscale and microscale skeletal changes. Specifically, Time-Domain Nuclear Magnetic Resonance (TD-NMR), Thermogravimetric Analysis (TGA), and synchrotron high-resolution powder X-ray diffraction (HRPXRD) analyses were performed. NMR measurements were performed on *P. damicornis* also from Dobu. In the $T_2$ distributions obtained by NMR (Supplementary Fig. S2), it was possible to identify a cut-off at 3 ms. This allowed to divide the pores containing water into two classes, distinguishing the smaller pores (smaller volumes, estimated pore sizes < 1 μm) from the remaining larger ones (larger volumes, estimated pore sizes > 1 μm). For the sake of simplicity, the two classes was named micro-scale and macro-scale pores [12,31]. The macro-scale pore volume fraction showed a 7% increase ($p < 0.05$) at the seep site compared to the control site only in Upa Upasina (Fig. 4; Supplementary Table S4). Figure 4 and Supplementary Table S5 summarize the intraskeletal organic matrix (OM) and water content (% mass loss) evaluated by TGA. In Dobu no significant difference between the control and seep sites was found neither for OM nor for water content ($p > 0.05$). In Upa Upasina, OM content showed a significant decrease in the seep compared to the control ($p < 0.01$), while a significant increase in water content was observed in the seep compared to the control ($p < 0.01$).

Three coral skeleton fragments of *P. damicornis* each from the control and seep sites in Upa Upasina were analysed by HRPXRD. All HRPXRD patterns were well indexed as aragonite and no additional diffraction peaks were detected. Then, they were refined using the Rietveld method [32] and lattice parameters and strain (Supplementary Table S6), and microstructural data [33], crystallite size, and microstrain (Supplementary Table S7), were calculated. No significant differences were found between the control and seep site. To test the influence of the OM on the mineral strain, *ex-situ* heat treatment prior the HRPXRD measurements were performed. The heat treatment removes the OM effects on the strain [34]. The data showed that the OM induced a positive strain on *a*- and *c*-axis and a negative one on the *b*-axis, but no significant differences were found between the control and seep site (Supplementary Table S6). We also measured crystallite size after the thermal annealing together with the transition to calcite (Supplementary Tables S6 and S7). These latter parameters did not show any significant difference between the control and seep sites.

## 3.3. Relations between variations of skeletal parameters and environmental variables

The DISTLM analysis exploring possible sources of variation in skeletal parameters of the single species related to the environmental parameters confirmed that *P. damicornis* was the species in which the environmental variables showed the strongest influence on skeletal parameters, as indicated by the higher proportion of variance explained, compared to the other two species (Supplementary Fig. S3). Massive *Porites* was excluded from the analysis since no significant changes in any of the measured skeletal

parameters were observed (Supplementary Fig. S3). The carbonate chemistry parameters explained almost all significant variations of skeletal parameters between locations and sites ($p < 0.05$; Table 2; Supplementary Fig. S3). In *P. damicornis*, also salinity contributed to explain some of the variance (Supplementary Fig. S3). For this species, the in-detail BEST BIO/ENV analyses on the multi-scale skeletal parameters (Supplementary Table S8) showed that $\Omega_{AR}$ and, in general, carbonate chemistry parameters, significantly correlated with most skeletal parameters. Moreover, salinity significantly correlated with changes in macro-scale pore volume fraction and intraskeletal water content, while temperature correlated with changes in intraskeletal OM content ($p < 0.05$; Supplementary Table S8).

# 4. Discussion

While measurable acidification of the tropical oceans has been underway for several decades now, detection and attribution of the effects of OA on reef-building corals has been challenging because multiple environmental changes, including ocean warming, are co-occurring with OA, impacting coral growth [35]. This study investigated the effects of long-term exposure to elevated $CO_2$ on skeletal properties in tropical zooxanthellate corals living at $CO_2$ vents.

Of the four species investigated, massive *Porites* was the only species showing unmodified skeletal parameters between seep and control sites at both locations. This is in agreement with a previous investigation performed at the same locations showing that the cover of massive *Porites* was twice as high at the seeps compared to the control sites, while net calcification and skeletal bulk density were similar [14]. Increased *Porite*s abundance and unchanged skeletal extension, skeletal bulk density, and net calcification rates with decreasing pH was also observed along a natural pH gradient in Palau [36]. Our results here corroborate the hypothesis that massive *Porites* spp have the capacity to acclimatize and thrive under persistent exposure to ocean acidification whereas any other and especially the structurally more complex branching corals appear to be more sensitive [23].

Similar to Mediterranean [12] and other tropical coral species [37], *G. fascicularis*, *A. millepora*, and *P. damicornis* showed a significant increase in porosity and decrease in bulk density at reduced $pH_{TS}$ in Upa Upasina. Although the Dobu seep site showed significantly higher $CO_2$ levels, with consequently lower pH and $\Omega_{AR}$ compared to the Upa Upasina seep, a significant increase of porosity and decrease of bulk density in the seep compared to the control site was observed only at Upa Upasina. This finding suggests that low pH is not the main driver and that other local environmental conditions not considered in this study interacted with OA to modify the skeletal parameters of these three coral species.

The species-specific DISTLM analyses and the BEST BIO/ENV analyses performed on *P. damicornis* pointed out that carbonate chemistry related parameters, in particular $\Omega_{AR}$, contributed to most of the observed changes for all species. This finding is in agreement with several studies showing a strong dependence of calcification on seawater aragonite saturation state [38]. Among the investigated species of the current study, only *P. damicornis* appears sensitive to the minor variation in salinity, which may indicate a trade-off between osmoregulatory and acid-base regulatory systems (controlling $H^+$ and $HCO_3^-$ uptake

from seawater), as observed in other calcifying marine organisms [39]. For example, responses of acid–base balance of crabs to both hypercapnia and changes in seawater salinity are related to iono-regulation because both homeostatic processes share the same mediators, such as $H^+$ and $HCO_3$- transporters [40]. *Pocillopora damicornis* exposed to hyposalinity conditions for 24 h showed decreased photosynthetic and respiratory activities [41]. Thus, this species may be more vulnerable to low pH under fluctuating salinities, a condition that is likely to occur in coastal environments in the face of global climate change [42]. Furthermore, *P. damicornis* was the only species displaying a variation in micro-density, with lower values at the seep site compared to the control. Micro-density, which represents the mass per unit volume of the biogenic calcium carbonate composing the skeleton [43], depends on the mineral composition of the skeleton and content of intraskeletal OM and water [26]. The additional analyses of macro- and micro- scale parameters performed in this species revealed an increase in macro-scale pore volume fraction and intraskeletal water content and a decrease in OM, and eventually strong linked water [28]. In particular, the observed increase in intraskeletal seawater content at the Upa Upasina seep can partially justify the observed decrease in skeletal micro-density. Changes in OM and water content with pH reduction are reported showing either increased content in the tropical *Stylophora pistillata* kept in aquaria at pH 7.2 for approximately one year [28,37], or no variation in the temperate *B. europaea* naturally living at a $CO_2$ vent [44]. However, it must be noted that different methodologies were used in the two studies. Transcriptomic data in aquaria experiments conducted on *A. millepora*, *P. damicornis*, and *S. pistillata* show that several genes encoding OM protein are up-regulated under reduced pH [45]. In particular, *P. damicornis* exposed to pH 7.8, 7.4 and 7.2 in aquaria for 3 weeks showed a 4 to 70-fold increase in up-regulation of genes encoding skeleton organic matrix proteins at all pH treatments [46].

The decrease in intra-skeletal OM in the samples from the seep site was not associated with a significant change in the strain, micro-strain, and crystallite size. These observations may indicate that the amount of intra-crystallite OM does not change, in agreement with the fact that the crystallite sizes after the thermal annealing are the same for samples from the control and the seep sites. Thus, the observed decrease in OM is likely associated with a decrease in the inter-crystallite OM. In addition, the stability of aragonite through the transition to calcite did not show a significant difference between control and seep samples, as well as the lattice parameters of the calcite formed after thermal annealing. The crystallographic features of aragonite from coral skeletons have been previously investigated [47]. The reef building coral *Stylophora pistillata* grown in aquaria under different experimental seawater acidification (pH 8.2, 7.6 and 7.3) showed anisotropic distortions of aragonite lattice parameters and a reduction of the crystallite sizes under acidified conditions [28]. In the presented study, these parameters were unaffected by decreasing pH, suggesting that biological control over calcification does not change at the nanoscale, as reported for *B. europaea* [12]. The fact that different species were used in a different experimental setting, field (life-long acclimatization) *vs* controlled conditions (short-term acclimation), account for these discrepancies. The calcite phase obtained by annealing of coral samples has similar lattice parameters in samples from the control and seep sites. These parameters, when compared with those of synthetic calcite [48], did not show differences. A different behavior was observed for calcite obtained from *Desmophyllum* and *Favia*

aragonitic skeletons, which showed different strain compared with geological or synthetic calcite [47]. In addition to the decreased OM, *P. damicornis* at the seep site of Upa Upasina also showed an increase of intra-skeletal seawater content, which could be partially related to the observed decrease of skeletal micro-density, but whose role in coral phenotypic plasticity to OA still has to be investigated. Again, these different responses seem species and environmental-specific.

# 5. Conclusions

This multi-species study showed that the combination of different environmental conditions can have a stronger effect on macro-scale skeletal parameters than average low pH values alone. Our findings showed a common phenotypic response among three zooxanthellate corals which all displayed a more porous skeletal phenotype under OA but also highlighted that OA is not always the main driver and that other local environmental conditions likely interacted with OA to determine the observed responses. Additionally, these skeletal macromorphological adjustments in *P. damicornis* did not affect the measured crystallite features, suggesting that the fundamental structural components produced by the biomineralization process might be substantially unaffected by increased acidification [12,49]. Nonetheless, the extra porous phenotype here described in the branching coral species may render structurally complex corals more vulnerable to damage and bio-erosion under climate change compared to massive growth forms [37,50], which in the future may lead to a weakening of the reef framework and subsequent degradation of the complex coral reef ecosystem. More generally, our findings highlight the importance of using a multi-parameter and multi-species analysis when investigating the vulnerability of coral species to OA, to understand what induces corals in a certain environment to acclimatize, and whether other species under the same conditions have the same capacity to adjust to future changes. These species and environmental specific differences highlighted in the present study contribute to explain the large range of responses to OA reported for corals and other marine calcifying organisms.

# Declarations

### Data Availability

The datasets generated during and/or analysed during the current study are available from the corresponding author on reasonable request.


### Acknowledgements

We would like to thank the communities at Upa Upasina and at Dobu to allow us to work at their unique reefs. Many thanks also to Craig Humphrey and Sam Noonan for collecting the samples. The field research was funded by the Australian Institute of Marine Science.


### Author contributions

KF designed the research, collected the specimens, and provided the background data. FP, LB, SF, IP, NB, FR, QP, BP, and LG analyzed the samples. FP, SF, SM, and PF performed the statistical analyses. FP, LB, PF, and

NB wrote the first draft. FP, LB, SF, NB, EC, ZD, PF, GF, and SG contributed to the scientific discussion and interpretation of the data. All authors contributed to writing the manuscript and gave final approval for publication.

### Additional Information

The authors declare that they have no competing interests.

# References


1. Hoegh-Guldberg, O. *et al.* Coral Reefs Under Rapid Climate Change and Ocean Acidification. *Science (80-.).* **318**, 1737–1742 (2007).
2. Roberts, M., Hanley, N., Williams, S. & Cresswell, W. Terrestrial degradation impacts on coral reef health: Evidence from the Caribbean. *Ocean Coast. Manag.* **149**, 52–68 (2017).
3. Mollica, N. R. *et al.* Ocean acidification affects coral growth by reducing skeletal density. Proc. Natl. Acad. Sci. 115, 1754–1759(2018).
4. Ries, J. B. Skeletal mineralogy in a high-CO2 world. *J. Exp. Mar. Bio. Ecol.* **403**, 54–64 (2011).
5. Erez, J., Reynaud, S., Silverman, J., Schneider, K. & Allemand, D. Coral calcification under ocean acidification and global change. *Coral Reefs: An Ecosystem in Transition.* https://doi.org/10.1007/978-94-007-0114-4_10 (2011).
6. Dove, S. G. *et al.* Future reef decalcification under a business-as-usual CO2 emission scenario. Proc. Natl. Acad. Sci. 110, 15342–15347(2013).
7. COOPER, T. F., DE'ATH, G. & LOUGH, J. M. Declining coral calcification in massive Porites in two nearshore regions of the northern Great Barrier Reef. *Glob. Chang. Biol.* **14**, 529–538 (2008).
8. Cooper, T. F., O'Leary, R. A. & Lough, J. M. Growth of Western Australian Corals in the Anthropocene. *Science (80-.).* **335**, 593–596 (2012).
9. Pandolfi, J. M. Incorporating Uncertainty in Predicting the Future Response of Coral Reefs to Climate Change. *Annu. Rev. Ecol. Evol. Syst.* **46**, 281–303 (2015).
10. Kroeker, K. J., Kordas, R. L., Crim, R. N. & Singh, G. G. Meta-analysis reveals negative yet variable effects of ocean acidification on marine organisms. *Ecol. Lett.* **13**, 1419–1434 (2010).
11. Jokiel, P. L. *et al.* Ocean acidification and calcifying reef organisms: a mesocosm investigation. *Coral Reefs.* **27**, 473–483 (2008).
12. Fantazzini, P. *et al.* Gains and losses of coral skeletal porosity changes with ocean acidification acclimation. *Nat. Commun.* **6**, 7785 (2015).
13. Wittmann, A. C. & Pörtner, H. O. Sensitivities of extant animal taxa to ocean acidification. *Nat. Clim. Chang.* **3**, 995–1001 (2013).
14. Fabricius, K. E. *et al.* Losers and winners in coral reefs acclimatized to elevated carbon dioxide concentrations. *Nat. Clim. Chang.* **1**, 165–169 (2011).
15. Riebesell, U. Acid test for marine biodiversity. *Nature.* **454**, 46–47 (2008).

16. Hall-Spencer, J. M. *et al.* Volcanic carbon dioxide vents show ecosystem effects of ocean acidification. *Nature.* **454**, 96–99 (2008).
17. Johnson, V. R., Russell, B. D., Fabricius, K. E., Brownlee, C. & Hall-Spencer, J. M. Temperate and tropical brown macroalgae thrive, despite decalcification, along natural CO 2 gradients. *Glob. Chang. Biol.* https://doi.org/10.1111/j.1365-2486.2012.02716.x (2012).
18. Prada, F. *et al.* Ocean warming and acidification synergistically increase coral mortality. *Sci. Rep.* **7**, 1–10 (2017).
19. Inoue, S., Kayanne, H., Yamamoto, S. & Kurihara, H. Spatial community shift from hard to soft corals in acidified water. *Nat. Clim. Chang.* **3**, 683–687 (2013).
20. Crook, E. D., Cohen, A. L., Rebolledo-Vieyra, M., Hernandez, L. & Paytan, A. Reduced calcification and lack of acclimatization by coral colonies growing in areas of persistent natural acidification. Proc. Natl. Acad. Sci. 110, 11044–11049(2013).
21. Teixidó, N. *et al.* Functional biodiversity loss along natural CO2 gradients. *Nat. Commun.* **9**, 5149 (2018).
22. Strahl, J. *et al.* Physiological and ecological performance differs in four coral taxa at a volcanic carbon dioxide seep. *Comp. Biochem. Physiol. Part A Mol. Integr. Physiol.* **184**, 179–186 (2015).
23. Fabricius, K. E., De'ath, G., Noonan, S. & Uthicke, S. Ecological effects of ocean acidification and habitat complexity on reef-associated macroinvertebrate communities. Proc. R. Soc. B Biol. Sci. 281, 20132479(2014).
24. Fabricius, K. E., Noonan, S. H. C., Abrego, D. & Harrington, L. De'ath, G. Low recruitment due to altered settlement substrata as primary constraint for coral communities under ocean acidification. Proc. R. Soc. B Biol. Sci. 284, 20171536(2017).
25. Noonan, S. H. C., Fabricius, K. E. & Humphrey, C. Symbiodinium Community Composition in Scleractinian Corals Is Not Affected by Life-Long Exposure to Elevated Carbon Dioxide. *PLoS One.* **8**, e63985 (2013).
26. Caroselli, E. *et al.* Environmental implications of skeletal micro-density and porosity variation in two scleractinian corals. *Zoology.* **114**, 255–264 (2011).
27. Borgia, G. C., Brown, R. J. S. & Fantazzini, P. Uniform-Penalty Inversion of Multiexponential Decay Data. *J. Magn. Reson.* **132**, 65–77 (1998).
28. Coronado, I., Fine, M., Bosellini, F. R. & Stolarski, J. Impact of ocean acidification on crystallographic vital effect of the coral skeleton. *Nat. Commun.* **10**, 2896 (2019).
29. R Development Core Team. R: A language and environment for statistical computing. *Vienna, Austria* (2018). doi:R Foundation for Statistical Computing, Vienna, Austria. ISBN 3-900051-07-0, URL http://www.R-project.org.
30. Anderson, M. J., Gorley, R. N. & Clarke, K. R. PERMANOVA + for PRIMER: Guide to Software and Statistical Methods. in Plymouth, UK(2008).
31. Fantazzini, P. *et al.* A Time-Domain Nuclear Magnetic Resonance Study of Mediterranean Scleractinian Corals Reveals Skeletal-Porosity Sensitivity to Environmental Changes. *Environ. Sci. Technol.* **47**,

12679–12686 (2013).

32. Toby, B. H. & Von Dreele, R. B. GSAS-II: the genesis of a modern open-source all purpose crystallography software package. *J. Appl. Crystallogr.* **46**, 544–549 (2013).
33. Jiang, H. G., Rühle, M. & Lavernia, E. J. On the applicability of the x-ray diffraction line profile analysis in extracting grain size and microstrain in nanocrystalline materials. *J. Mater. Res.* **14**, 549–559 (1999).
34. Pokroy, B., Fitch, A. & Zolotoyabko, E. The Microstructure of Biogenic Calcite: A View by High-Resolution Synchrotron Powder Diffraction. *Adv. Mater.* **18**, 2363–2368 (2006).
35. Vercelloni, J. *et al.* Forecasting intensifying disturbance effects on coral reefs. *Glob. Chang. Biol.* **26**, 2785–2797 (2020).
36. Barkley, H. C. *et al.* Changes in coral reef communities across a natural gradient in seawater pH. *Sci. Adv.* **1**, e1500328–e1500328 (2015).
37. Tambutté, E. *et al.* Morphological plasticity of the coral skeleton under CO2-driven seawater acidification. *Nat. Commun.* **6**, 7368 (2015).
38. Hoegh-Guldberg, O., Poloczanska, E. S., Skirving, W. & Dove, S. Coral Reef Ecosystems under Climate Change and Ocean Acidification.*Front. Mar. Sci.***4**, (2017).
39. Charrieau, L. M. *et al.* Decalcification and survival of benthic foraminifera under the combined impacts of varying pH and salinity. *Mar. Environ. Res.* **138**, 36–45 (2018).
40. Ramaglia, A. C., de Castro, L. M. & Augusto, A. Effects of ocean acidification and salinity variations on the physiology of osmoregulating and osmoconforming crustaceans. *J. Comp. Physiol. B.* **188**, 729–738 (2018).
41. Gardner, S. G. *et al.* Dimethylsulfoniopropionate, superoxide dismutase and glutathione as stress response indicators in three corals under short-term hyposalinity stress. Proc. R. Soc. B Biol. Sci. 283, 20152418(2016).
42. Fujii, T. & Climate Change Sea-Level Rise and Implications for Coastal and Estuarine Shoreline Management with Particular Reference to the Ecology of Intertidal Benthic Macrofauna in NW Europe. *Biology (Basel).* **1**, 597–616 (2012).
43. Barnes, D. J. & Devereux, M. J. Variations in skeletal architecture associated with density banding in the hard coral Porites. *J. Exp. Mar. Bio. Ecol.* **121**, 37–54 (1988).
44. Goffredo, S. *et al.* Biomineralization control related to population density under ocean acidification. *Nat. Clim. Chang.* **4**, 593–597 (2014).
45. Zoccola, D. *et al.* Coral Carbonic Anhydrases: Regulation by Ocean Acidification. *Mar. Drugs.* **14**, 109 (2016).
46. Vidal-Dupiol, J. *et al.* Genes related to ion-transport and energy production are upregulated in response to CO2-driven pH decrease in corals: new insights from transcriptome analysis. *PLoS One.* **8**, e58652 (2013).
47. Stolarski, J., Przeniosło, R., Mazur, M. & Brunelli, M. High-resolution synchrotron radiation studies on natural and thermally annealed scleractinian coral biominerals. *J. Appl. Crystallogr.* **40**, 2–9 (2007).

48. Maslen, E. N., Streltsov, V. A., Streltsova, N. R. & Ishizawa, N. Electron density and optical anisotropy in rhombohedral carbonates. III. Synchrotron X-ray studies of CaCO 3, MgCO 3 and MnCO 3. *Acta Crystallogr. Sect. B Struct. Sci.* **51**, 929–939 (1995).
49. Wall, M. *et al.* Linking Internal Carbonate Chemistry Regulation and Calcification in Corals Growing at a Mediterranean CO2 Vent.*Front. Mar. Sci.***6**, (2019).
50. Reyes-Nivia, C., Diaz-Pulido, G., Kline, D., Guldberg, O. H. & Dove, S. Ocean acidification and warming scenarios increase microbioerosion of coral skeletons. *Glob. Chang. Biol.* **19**, 1919–1929 (2013).

# Tables

Table 1

Means and standard deviation (in parenthesis) of the investigated environmental parameters in seep and control sites in Dobu and Upa Upasina. T-test results between controls and seeps at each location are reported in bold, *** P < 0.001. T-test results between control sites and between seep sites of the two locations are reported on the last column to the right.

| **Location** | **Dobu** | | **Upa Upasina** | | **t-test between sites** | |
|---|---|---|---|---|---|---|
| Site | Control | Seep | Control | Seep | Controls | Seeps |
| $pH_{TS}$ | 7.96 (0.04) | 7.66*** (0.27) | 7.91 (0.13) | 7.75*** (0.19) | P = 0.009 | P = 0.001 |
| | N = 46 | N = 130 | N = 67 | N = 222 | | |
| $pCO_2$ ($\mu$atm) | 463 (65) | 1381*** (1375) | 555 (316) | 989*** (990) | P = 0.054 | P = 0.005 |
| | N = 46 | N = 130 | N = 67 | N = 222 | | |
| $\Omega_{AR}$ | 3.39 (0.36) | 2.15*** (0.88) | 3.29 (0.70) | 2.52*** (0.71) | P = 0.389 | P = 0.000 |
| | N = 46 | N = 130 | N = 67 | N = 222 | | |
| DIC ($\mu$mol $kg^{-1}$) | 1946 (15) | 2106*** (90) | 2082 (38) | 2060*** (30) | P = 0.000 | P = 0.009 |
| | N = 32 | N = 30 | N = 71 | N = 254 | | |
| TA ($\mu$mol $kg^{-1}$) | 2235 (9) | 2275*** (0.97) | 2252 (21) | 2285*** (18) | P = 0.000 | P = 0.000 |
| | N = 47 | N = 207 | N = 71 | N = 254 | | |
| Salinity (‰) | 34.9 (0.79) | 34.7 (0.72) | 35.1 (0.75) | 34.8*** (0.65) | P = 0.026 | P = 0.072 |
| | N = 59 | N = 207 | N = 71 | N = 254 | | |
| T (°C) | 29.1 (1.41) | 29.0 (0.72) | 30.1 (1.29) | 30.2 (0.94) | P = 0.000 | P = 0.000 |
| | N = 59 | N = 207 | N = 71 | N = 242 | | |

$pH_{TS}$: pH in total scale; $pCO_2$: carbon dioxide partial pressure; $\Omega_{AR}$: aragonite saturation; DIC: dissolved inorganic carbon; TA: Total Alkalinity; T = seawater temperature. P: significance of t-test; N: number of measurements

Table 2

Detailed results of the DISTLM analyses and tests of marginality to explore trends of biological parameters with environmental variables reported in Supplementary Figure S3. DISTLM used the BEST selection procedure and adjusted $R^2$ selection criteria. Values of P indicate level of statistical significance related to the result. Significant values are reported in bold.

| | **A. millepora** | | **G. fascicularis** | | **Massive Porites** | | **P. damicornis** | |
|---|---|---|---|---|---|---|---|---|
| Variable | Proportion of variance explained | P | Proportion of variance explained | P | Proportion of variance explained | P | Proportion of variance explained | P |
| Salinity | 0.06 | 0.09 | 0.07 | 0.139 | 0.17 | 0.006 | 0.16 | 0.009 |
| Temperature | 0.00 | 0.89 | 0.03 | 0.303 | 0.02 | 0.46 | 0.04 | 0.261 |
| TA | 0.07 | 0.03 | 0.04 | 0.234 | 0.18 | 0.004 | 0.16 | 0.012 |
| DIC | 0.00 | 0.68 | 0.03 | 0.334 | 0.07 | 0.101 | 0.01 | 0.79 |
| $pH_{TS}$ | 0.10 | 0.01 | 0.09 | 0.084 | 0.17 | 0.005 | 0.21 | 0.002 |
| $pCO_2$ | 0.12 | 0.01 | 0.08 | 0.089 | 0.15 | 0.012 | 0.22 | 0.003 |
| $\Omega_{AR}$ | 0.11 | 0.01 | 0.11 | 0.060 | 0.15 | 0.012 | 0.21 | 0.005 |

# Figures

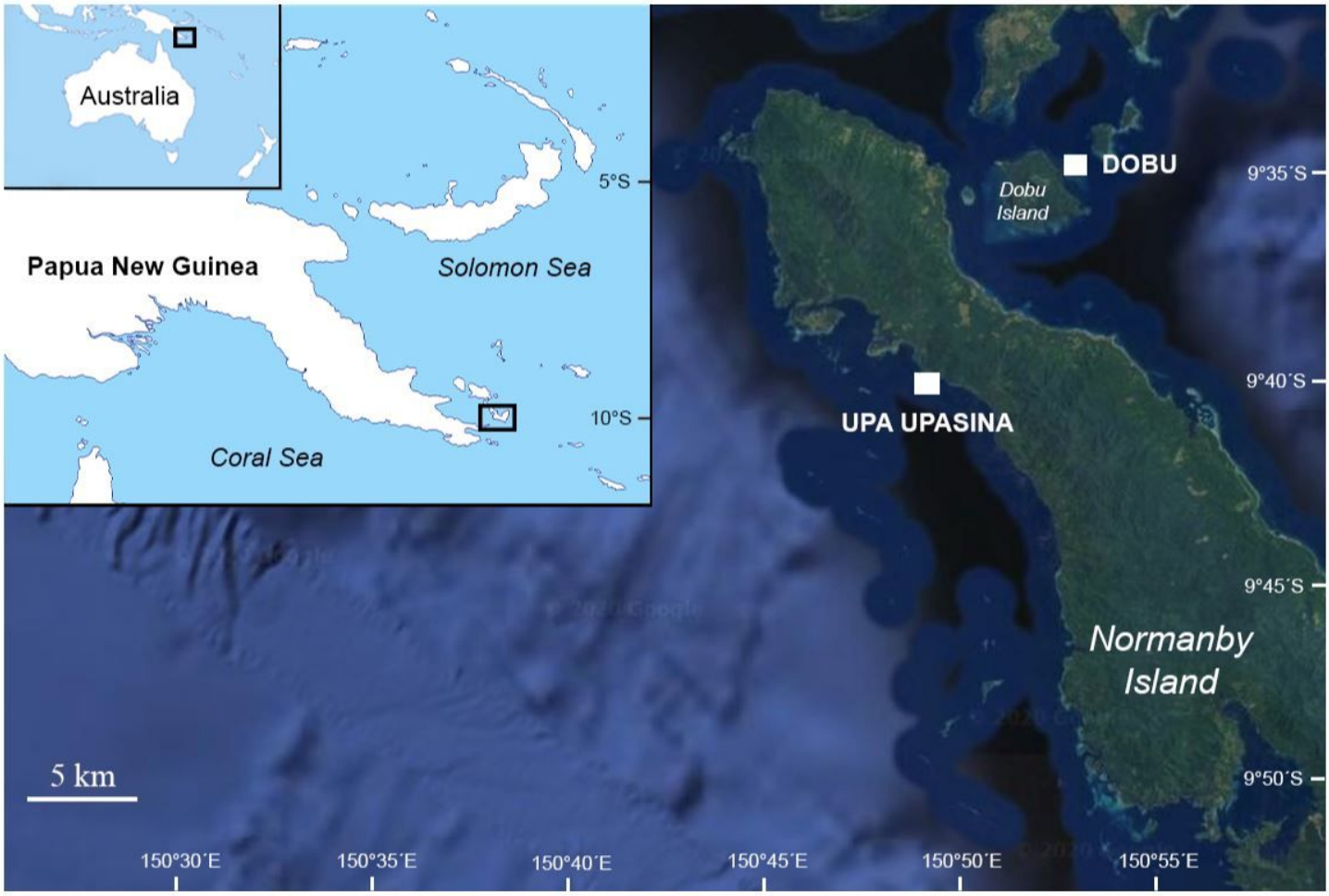


## Figure 1

Maps of Papua New Guinea and the two study locations (Dobu and Upa Upasina) on Normanby and Dobu Islands, Milne Bay Province. Note: The designations employed and the presentation of the material on this map do not imply the expression of any opinion whatsoever on the part of Research Square concerning the legal status of any country, territory, city or area or of its authorities, or concerning the delimitation of its frontiers or boundaries. This map has been provided by the authors.

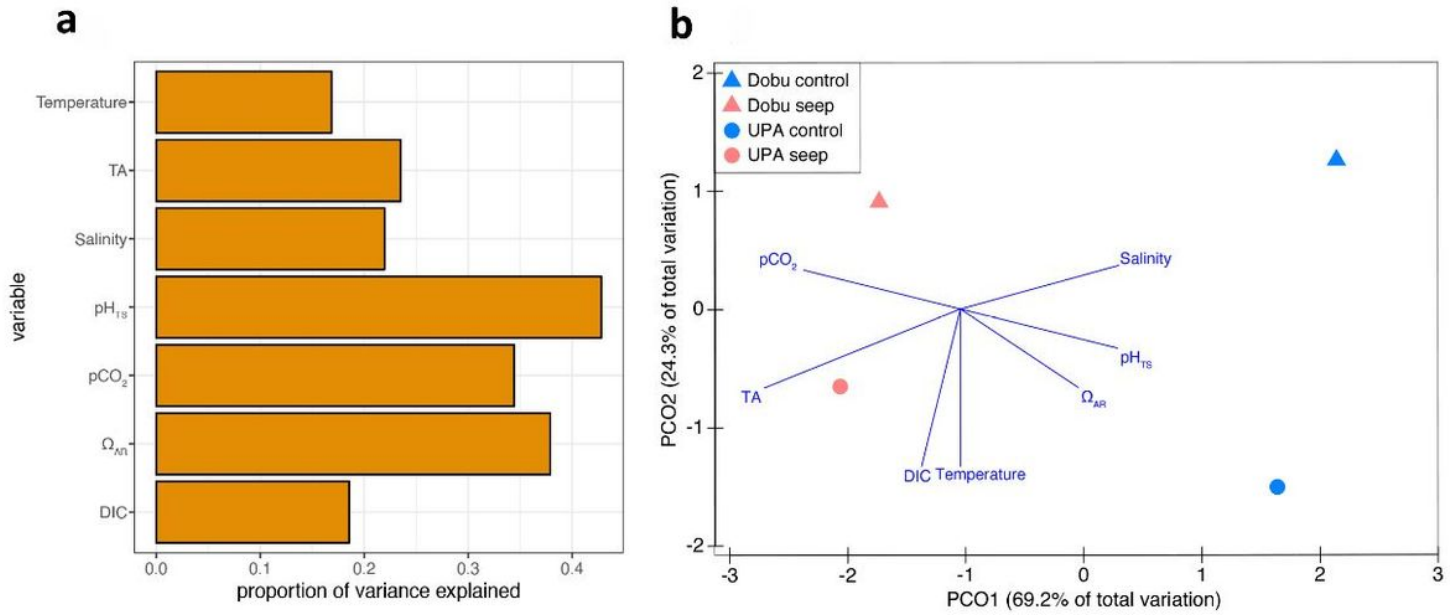


## Figure 2

(A) Results from the test of marginality related to the distance-based redundancy (DISTLM) analysis showing contribution of each environmental variable to the total variance observed in environmental dataset. DISTLM used the BEST selection procedure and adjusted R2 selection criteria. Contribution of all variables has level of statistical significance $p < 0.01$ according to the test of marginality. (B) Principal coordinates ordination (PCO) bi-plot of whole environmental dataset variation amongst sampling locations and sites (Euclidean Distance resemblance matrix; 999 permutations). Only average values are displayed in the bi-plot, while the statistical inference was performed on the whole dataset. Vectors for the environmental variables to be displayed in the bi-plot were filtered according to their Spearman correlation's coefficients ($r > 0.7$ with at least PCO1 or PCO2).

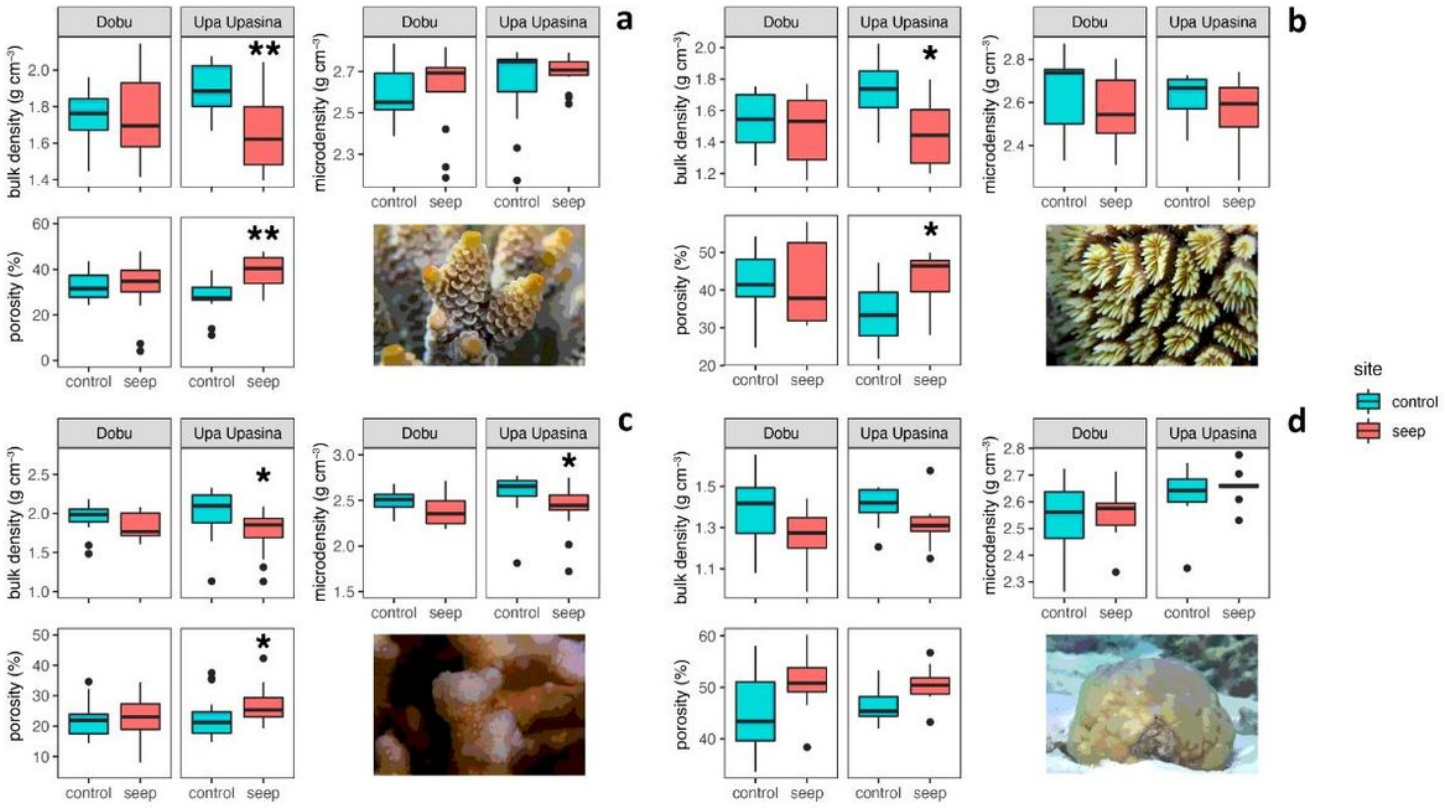


## Figure 3

Skeletal parameters micro-density, porosity and bulk density at control (green box plots) and seep sites (pink box plots) in Dobu and Upa Upasina (UPA) for (A) Acropora millepora, (B) Galaxea fasciularis, (C) Pocillopora damicornis, and (D) Massive Porites. Significant differences between control and seep sites are represented by asterisks, ** p<0.01, * p<0.05. The box indicates the 25th and 75th percentiles and the line within the box marks the median. Whisker length is equal to 1.5 × interquartile range (IQR). Circles represent outliers.

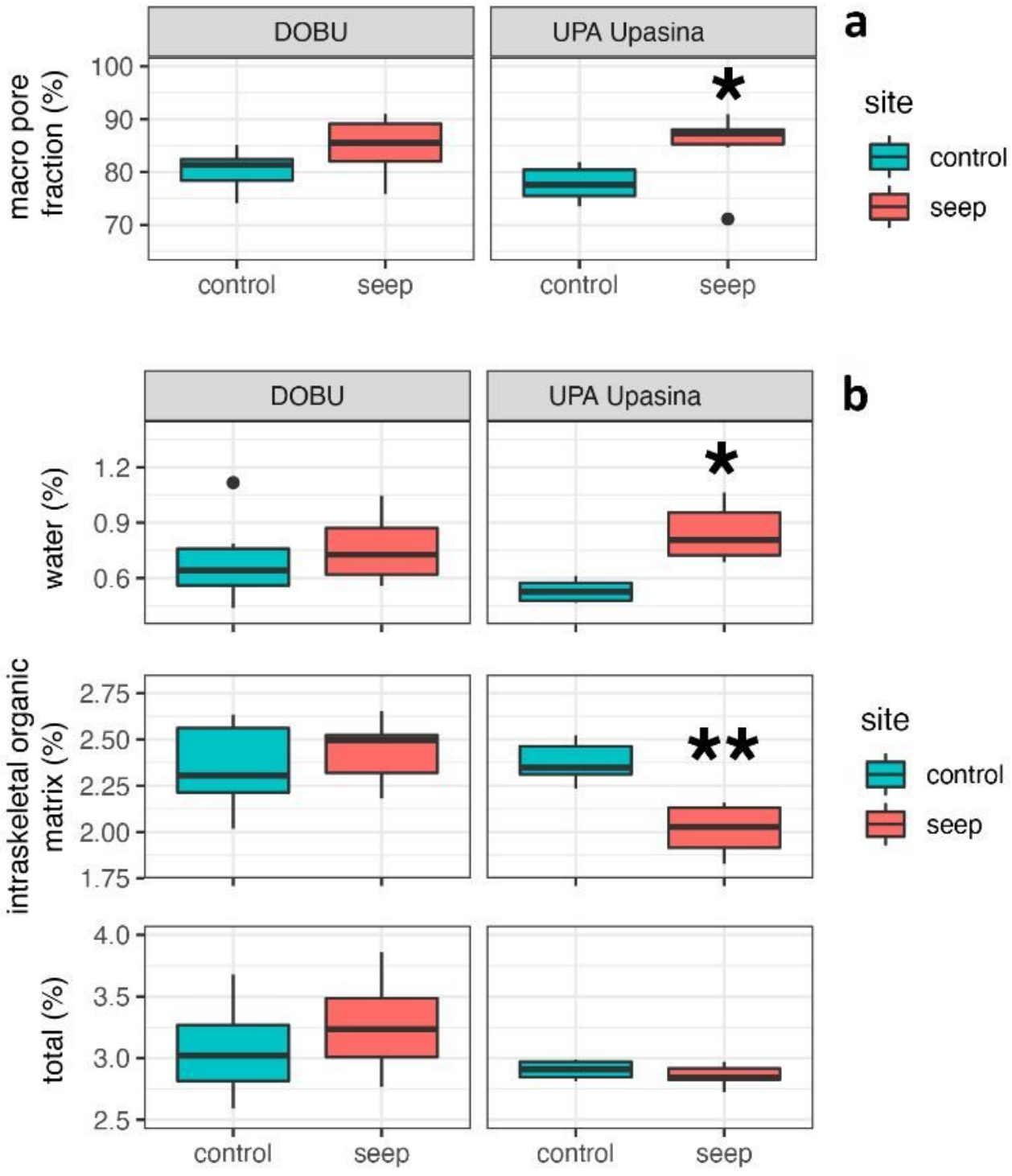


**Figure 4**

Macro-scale pore volume fraction (in the figure simply macro pore fraction) and intraskeletal OM and water content for P. damicornis from control and seep sites at Dobu and Upa Upasina. (A) TD-NMR measurement of macro-scale pore volume fraction. (B) TGA measurements of microscale parameters, namely intraskeletal organic matrix (OM), intraskeletal water content, and total (the sum of OM and water). The box indicates the 25th and 75th percentiles and the line within the box marks the median. Whisker length is

equal to 1.5 × interquartile range (IQR). Circles represent outliers. Significant differences between control and seep sites are represented by asterisks, ** $p<0.01$, * $p<0.05$.

## Supplementary Files

This is a list of supplementary files associated with this preprint. Click to download.

- SupplementaryMaterialSciRep30122020.pdf